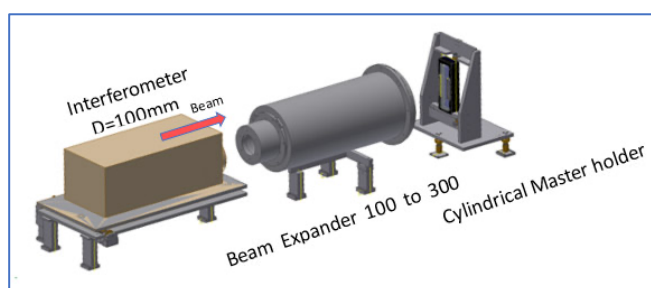


AHEAD 2020 Scientific/Technical Report - WP no. 10

Deliverable n. 10.4

Advancement on the new high-precision metrology systems for testing X-ray optics



Issued by	Bianca Salmaso¹ Mauro Ghigo¹	WP10.2 Task leader WP10.2 Beam expander subtask leader
Approved by	Gianpiero Tagliaferri¹	WP10.2, WP10.1 Management support
Contributors	S. Basso¹, V. Cotroneo¹, M. Ghigo¹, G. Pareschi¹, G. Sironi¹, D. Sisana¹, D. Spiga¹, G. Vecchi¹	
Affiliation	¹ INAF – Osservatorio Astronomico Brera, Italy	

Project acronym:
AHEAD2020

Project Title:
Integrated Activities for the High Energy Astrophysics Domain

Grant Agreement No: **871158**

This deliverable is part of a project that has received funding from the European Union's Horizon 2020 research and innovation programme

Start date of the project:
2022-02-01

Version	Revision Date	Review/Approval
01 – draft	01 Feb 2022	All

Distribution List	AHEAD2020 Management Team (bold font indicates task leaders)	
	Vadim Burwitz	WP10.0, WP10.1, WP10.3
	Charly Feldman	WP10.1, WP10.3
	René Hudec	WP10.1
	Bianca Salmaso	WP10.1, W10.2
	Gianpiero Tagliaferri	WP10.1, W10.2
	Paul O’Brien	WP10.1, W10.3
	Giovanni Pareschi	WP10.1, W10.2
	Dick Willingale	WP10.1, W10.3

Contents

1.	SCOPE	4
2.	BEATRIX	4
2.1	INTRODUCTION	4
2.2	DESCRIPTION OF THE SYSTEM	5
2.3	THE X-RAY BEAM	11
2.4	PROGRAMMED ACTIVITIES AND SCHEDULE	12
3.	BEAM EXPANDER FOR INTERFEROMETRIC MEASUREMENTS	13
3.1	INTRODUCTION	13
3.2	PERFORMED ACTIVITIES	14
3.2.1.	<i>MANUFACTURING OF THE MECHANICAL COMPONENTS.....</i>	<i>14</i>
3.2.2.	<i>MEASUREMENTS OF THE BEAM EXPANDER OPTICAL TRAIN BEFORE IBF</i>	<i>16</i>
3.2.3.	<i>MEASUREMENTS OF THE CYLINDRICAL LENSES WITH CMC 3D MACHINE</i>	<i>16</i>
3.2.4.	<i>IBF UPGRADE</i>	<i>17</i>
3.3	PROGRAMMED ACTIVITIES AND SCHEDULE	18

1. Scope

This document presents the advancement status on the deliverable D10.4 “Report on new high precision metrology systems for testing X-ray optics” for the Task 10.2 “Development of optics for the beam conditioning in future calibration facilities and high precision metrology (INAF/OAB, MPG)”. The goal of this task is to complete two metrology systems in the Merate premise of the INAF - Osservatorio Astronomico di Brera:

1. BEaTriX, the Beam Expander Testing X-ray facility: to test X-ray optics with an expanded X-ray beam
2. Beam Expander for Interferometric measurements: to measure interferometrically the shape of an X-ray optic with an high quality expanded cylindrical beam of coherent visible light

Due to the Covid emergency, these instruments are not completed yet. The energies of the OAB staff were concentrated into the BEaTriX facility which is now in the commissioning phase, and is expected to be soon completed in Q1 2022. On the other hand, the interferometric facility advancements were slower. In this report, we present the status of both systems, clarifying what is reached and what is still needed. The final report will be submitted in one year time, by 2023 Feb. 01.

2. BEaTriX

2.1 Introduction

INAF/OAB is building, at its premises in Merate, the BEaTriX (Beam Expander Testing X-ray) test facility, with the prime goal to prove that it is possible to perform the acceptance tests (PSF and Aeff) of the ATHENA Silicon Pore Optics (SPO) Mirror Modules (MM) at its production rate. The project was at first financed by the AHEAD grant #654215, then it was financed by ESA with significant contributions also by ASI and INAF, and now also by the AHEAD-2 grant #871158.

The ATHENA X-ray telescope comprises an optical system with several hundreds of SPO MM's to be assembled. All the MMs have to be tested for acceptance before integration. For a fast and precise testing, the BEaTriX facility was designed as a compact facility with fast vacuum pump-down, and with a broad beam to fully illuminate the aperture of the MMs. The beam is 170 mm × 60 mm wide, uniform, parallel (divergence ≤ 1.5 arcsec HEW), with energy of 4.51 keV, for the first beam line, and 1.49 keV for the second beam line to be added later.

The optical and mechanical designs of BEaTriX are shown in Fig. 1: X-rays are emitted by an X-ray microfocus source with a Titanium anode (A), are propagated through a vacuum tube (B), named Short Arm (SA1) and reflected by a paraboloidal mirror (C); the beam is then diffracted by the monochromator stage with 4 symmetrically cut crystals (D), and by an expansion stage made by an asymmetrically-cut crystal (E)). The mirror and the crystals are enclosed in a chamber named Optical Chamber (OC). The beam is then collected by the MMs under test, present in the chamber (F) named Mirror Module Chamber (MMC), and focused on a directly-illuminated CCD camera placed at a 12 m distance (H), which is connected to the MMC with a vacuum tube (G) named Long Arm (LA).

Among the optical components, the parabolic mirror has been polished and figured entirely at INAF/OAB-Merate. The work done on this mirror was presented in the deliverable D 10.1 “Report on the beam conditioning optics for test facilities”.

This report presents the status of the facility as built, with special focus on the X-ray beam characteristics.

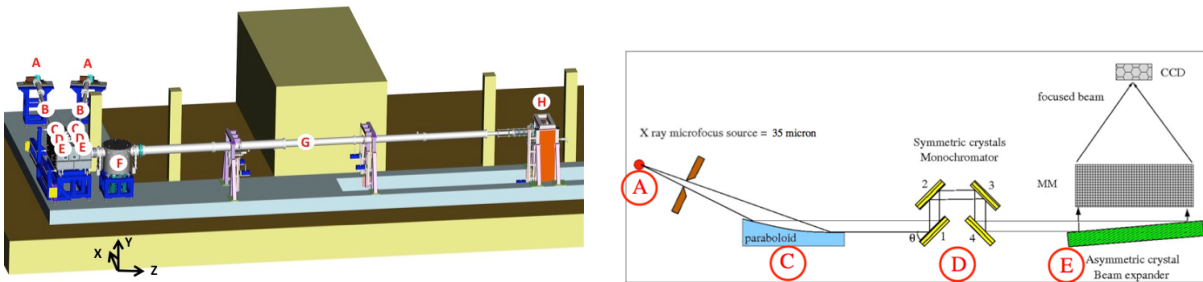


Figure 1: BEaTriX: mechanical design (left), and optical design (right)

2.2 Description of the system

As X-rays of 4.5 and 1.5 keV are absorbed in air, the beam is propagated in a vacuum system. The entire system (Fig. 2) is positioned on a stable foundation, designed and built to isolate the beam line from vibrations. The system is very compact ($9 \times 18 \text{ m}^2$) and this contributes to reduce the evacuation time with respect to bigger X-ray facilities. The facility is divided into 4 modular compartments by gate valves, in order to have the possibility to operate the vacuum/venting independently. In particular, the MM Chamber can be isolated by two gate valves, for a fast MM replacement.



Figure 2: The BEaTriX vacuum system positioned over the isolated foundations

The primary vacuum is accomplished by oil-free pre-vacuum and backing pumps, to avoid contamination of the optics. The primary pumps are placed outside the foundations to avoid vibrations (Fig. 3 left). The low vacuum (10^{-6} mbar) is reached with magnetically levitated turbomolecular pumps: as they are flanged to the vacuum system (Fig. 3 center), the magnetic levitation of the rotors was chosen to have low vibration operation.

Vacuum sensors and electro-valves are available all along the beam line to monitor the vacuum status (Fig. 3 right).

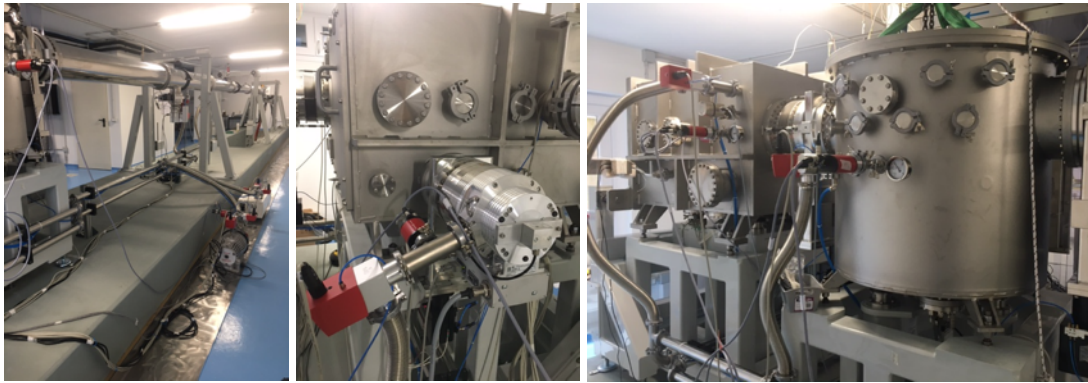


Figure 3: Left: The primary pumps, placed outside the foundations. Centre: the turbomolecular pump of the Optical Chamber. Right: some of the vacuum sensors and electro-valves used to operate the vacuum.

Venting is performed in all the system with dried dehumidified air. Compressed air is arriving from a main compressor, already present in OBA to serve several laboratories. The air is filtered by a dedicated system (Fig. 4) and it was certified to be in line with the BEaTriX requirement: particles comparable with ISO6 clean room, dew point lower than the operation temperature of the detector (-20°C), oil content $< 0.015 \text{ mg/m}^3$.



Figure 4: Left: The filtering system for the air used for venting. Right: A small stainless-steel tank is placed close to the clean tent to have clean dry air available for the optics cleaning, if needed

The experimental chamber opens into an ISO5 clean tent (Fig. 5), to allow samples to be loaded and unloaded in a clean environment.

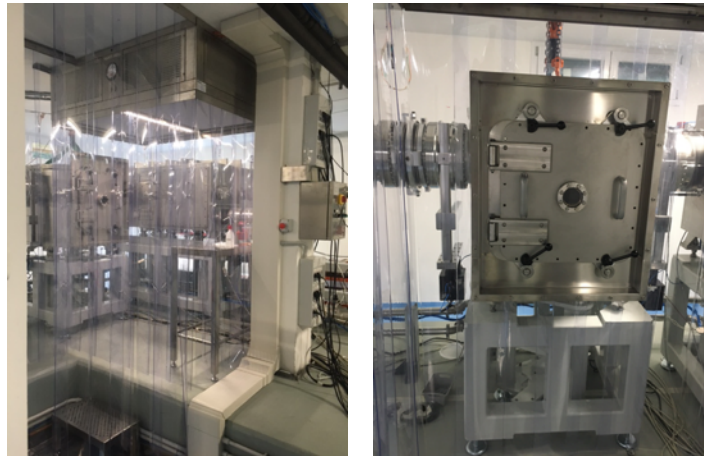


Figure 5: Left: the ISO5 clean tent. Right: the door of the MM Chamber from the clean tent

A thermal box is also present to radiatively heat the X-ray optics under test, in the temperature range $T=293\pm 25\text{K}$ (Fig. 6).



Figure 6: Left: the thermal box cover with UHV Al foil. Centre: the chiller connected to the thermal box via feedthroughs. Right: the thermal box inside the MM Chamber [PR#35]

The X-ray source for the 4.5 keV beam line is a micro-focus source with titanium anode (Fig. 7 left), enclosed in a shielding box that avoid X-ray leaks in the operation environment (Fig. 7 center). The source, with focal spot of $35 \times 35 \mu\text{m}$, is in UHV environment, separated by a $100 \mu\text{m}$ thick Be window. The flux of the Ti source was measured to be 6×10^{11} ph/sec/sterad. An Si-PIN detector (Amptek, X123 with 25mm^2 area / $500 \mu\text{m}$ thickness / $25 \mu\text{m}$ Be window) monitors the flux stability and the stability of the aligned components.

The source is placed on a manipulator (Fig. 7 right) that assists the alignment of the source itself with respect to the paraboloidal mirror.

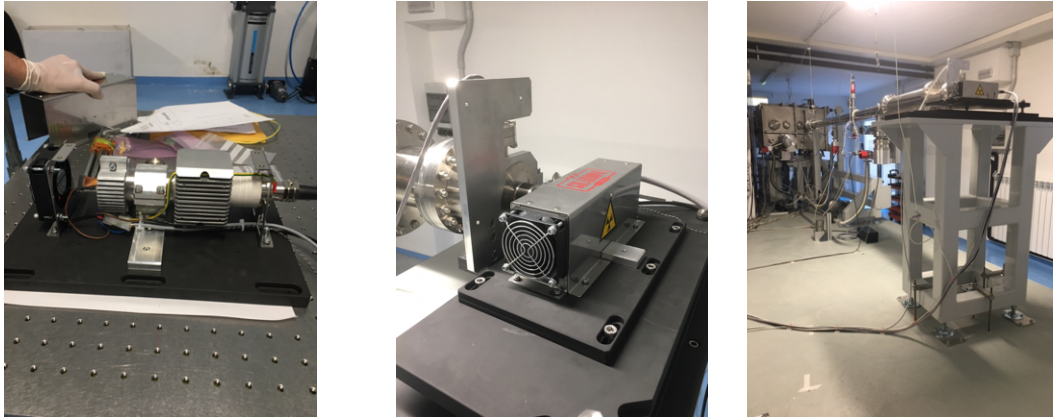


Figure 7: The X-ray tube with fan and radiators (left), mounted with the X-ray shield on its manipulator (center), positioned on the source tower (right)

The paraboloidal mirror was entirely polished at INAF-OAB: the work was reported in a previous deliverable [D10.1]. The quality of the mirror was tested in X-rays at the PANTER X-ray facility (Fig. 8), before and after coating with a bi-layer of Cr (4.6 nm) and Pt (30 nm). The result was nicely in line with the simulations, giving an HEW of about 3 arcsec, as measured with a parallel beam configuration at 1.49 keV.

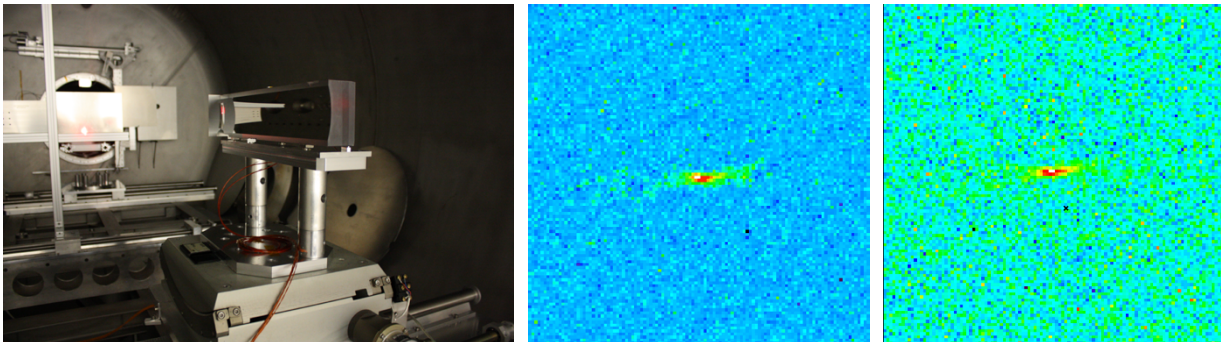


Figure 8: Left) the BEaTriX paraboloidal mirror mounted in the PANTER vacuum chamber, viewed from the detectors side. Center) Best focus measured with PIXI at 1.49 keV in parallel setup, before coating, HEW = 3.1 arcsec. Right) Same as previous image but after coating, HEW = 2.8 arcsec.

After the collimation, the beam is filtered tightly in energy to ensure the final collimation of the expanded beam. This is obtained via a 4-fold diffraction on silicon crystals, cut parallel to the (220) planes (Fig. 9 left). After emerging from the monochromators, the beam is diffracted at about 90 deg by another silicon crystal, asymmetrically cut with respect to the (220) planes (Fig. 9 right), in order to ensure an expansion of about 50 times. The monochromator can optimize either the horizontal divergence or the flux: two different configurations can in principle be adopted one in which the vertical divergence only is optimized (max flux), and one in which both vertical and horizontal divergences play a key role and need to be optimized (low flux).

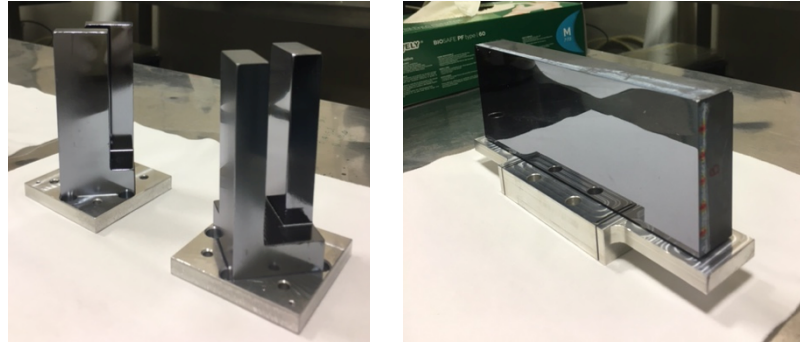


Figure 9: The Si [220] crystals for the monochromator (left) and beam expansion (right)

The detector is an iKon-L from Andor, Model DW936R, mounting a 2048x2048 pixels (13.5 μm x 13.5 μm pixel size) back-illuminated sensor from E2V, model CCD42-40, in open configuration. It is flanged at 12 m distance from the MM (Fig. 10 left). A cold finger is present in front of the CCD sensor, to protect the sensor from any possible condensation: the cold finger operates at -30°C while the CCD at -20°C .

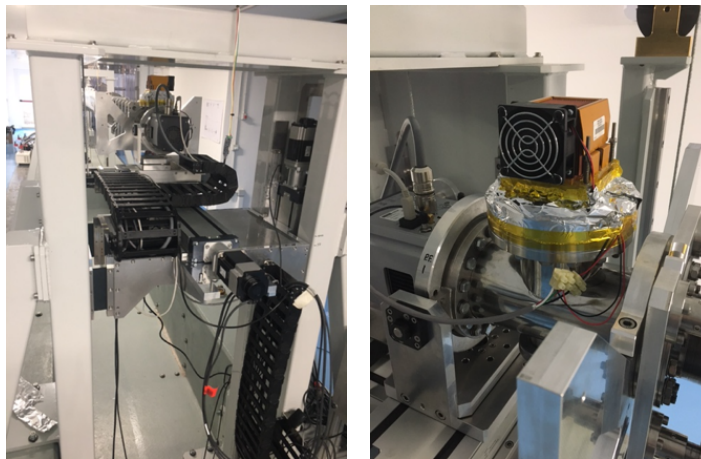


Figure 10: Left: the CCD flanged at the end of the long arm. Right: the cold finger flanged in front of the CCD

The components in charge of the beam moderation are positioned over vacuum motors inside the OC (Fig. 11). The parabolic mirror can be aligned in pitch and yaw. The crystals can be aligned in pitch, roll and are mounted over a translational stage to move them in and out from the beam when needed (for instance during alignment). Close to each component, PT100 sensors monitor their temperature.

In the MMC, the MM is motorized in vacuum (Fig. 12) in order to be aligned to the beam: a hexapod (H-824-G2V by Physik Instrumente), with max load of 5kg, is used for this purpose. The hexapod is mounted on a translational stage, used to bring a reference area into the beam for the Effective Area measurements. In these cases, three PT100 sensors monitor the temperature of the bottom and top of the hexapod and the temperature at the MM level. These sensors have shown a temperature increase at the base of the hexapod of only 5°C , with no significant increase at the MM level, owing to its insulating support (Fig. 16).

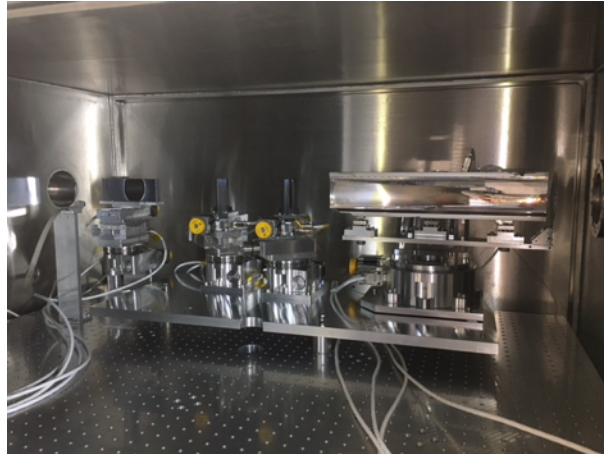


Figure 11: The Optical Chamber: from right to left, the parabolic mirror, the two channel cut crystals used as monochromator, and the crystal for the beam expansion, positioned on their motorization needed for the alignment.

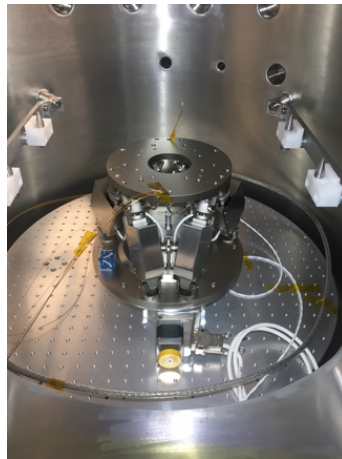


Figure 12: The Mirror Module Chamber: the hexapod is visible, mounted over a translational stage used to bring a reference area in and out the beam.

Special attention was dedicated to the design of the detector tower, that hosts the detector and its motorizations (Fig. 13). The detector moves on three linear stages. The travel ranges of the stages are: range-Z = 600 mm (for the focus search), range-Y = 1500 mm (for the vertical displacement of the image for MMs of different radii), range-X = 200 mm (for the qualification of the beam).

The detector is connected to the vacuum system by a bellow to enable the focus search. The 12 m long arm is made of 6 tubes to leave the possibility to modify in the future the focal length of the facility: major setup changes will be necessary but in principle focal distances other than 12 m are possible ($f_{\text{std}} = 12000 \pm 250$ mm; $f_{\text{possible-1}} = 10295 \pm 250$ mm; $f_{\text{possible-2}} = 8295 \pm 250$ mm).



Figure 13: The detector tower. Left: holes to anchor the tower are prepared at $f = 12 - 10 - 8$ m, for flexibility of the facility. Right: The tower with the bellow for the focus search.

2.3 The X-ray beam

The qualification of the beam is performed with an ad-hoc produced Hartmann plate, with $400 \mu\text{m}$ square holes, installed in the MM Chamber (Fig. 14).

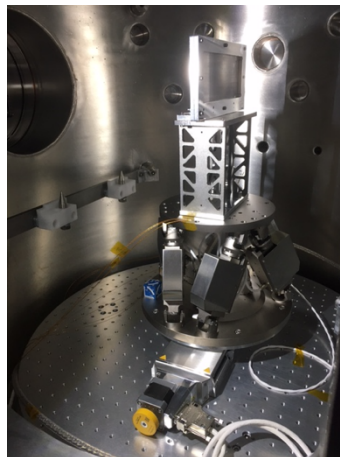


Figure 14: The Hartmann plate installed on the support that will be used also for the MMs, and positioned over the hexapod

Two components of the divergence are obtained and added in quadrature to have the final HEW:

- 1) Low frequency errors (misalignment of the optical components + low frequency errors of the parabolic mirror) are computed by the deviation of the centroid of each hole from its nominal position. A scan of the parallel beam, in a field $150 \text{ mm} \times 60 \text{ mm}$, has been acquired (Fig. 15).

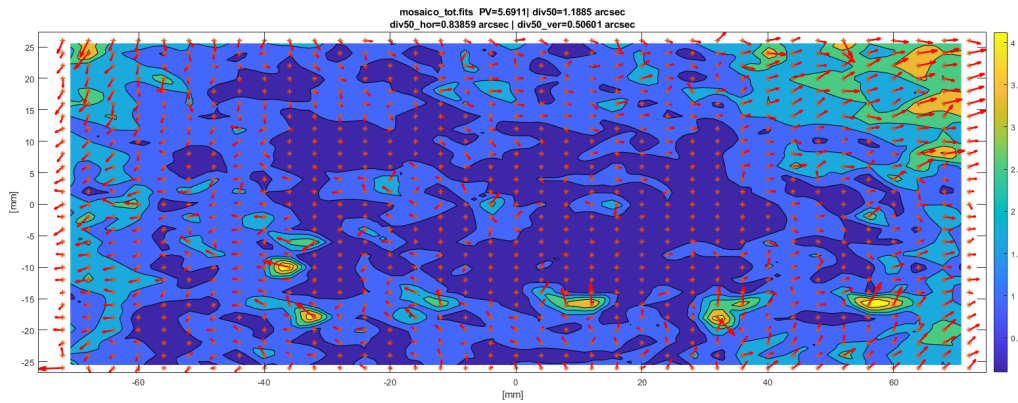


Figure 15.: Divergence computation on the composition of 3x7 images taken with the Hartmann plate with 400um holes

2) The contribution of the source finite size, the dispersion of the beam expander and the high frequency of the parabolic mirror, have an impact over the lateral scale of each single hole. Fig. 16 shows the contribution to the divergence obtained from these data.

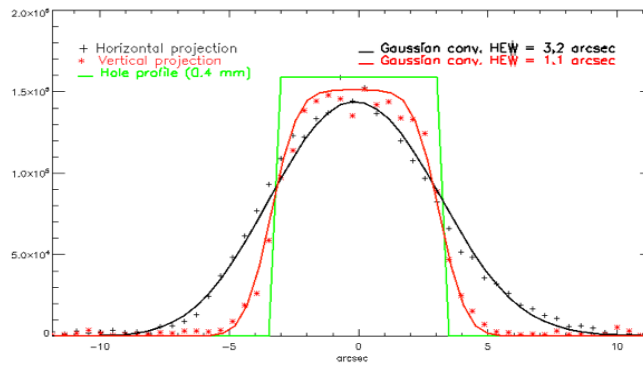


Figure 16: Intensity profiles inside the hole, obtained with the optimized par-pitch position

Considering the quadrating sum of the two contributions from the baricenter of the holes (Fig. 15) and the intensity inside the holes (Fig. 16), the total divergence of the beam is computed in the configuration of no rotation for the CCC2 (high divergence / high flux):

$$\begin{aligned} \text{HEW}_{\text{HOR}} &= 3.6 \text{ arcsec} \\ \text{HEW}_{\text{VER}} &= 1.5 \text{ arcsec} \end{aligned}$$

The result shows the vertical HEW to be in line with the requirement. The horizontal HEW will be decreased using the monochromator in the configuration of low divergence / low flux, which is accomplished by a rotation of the CCC2.

2.4 Programmed activities and schedule

In the next future the following activities will be performed to fully qualify the beam:

- optimization of the horizontal HEW by rotation of the CCC2;
- optimization of the uniformity by dithering the beam expander crystal back and forth in Z axis;
- stability of the beam.

After these activities, the X-ray beam will be fully characterized and the facility ready to be tested on a reference MM, measuring the PSF and Effective Area. This is expected to be completed by Q1 2022.

Some work for the second beam line at the 1.5 keV energy is already started, such as the figuring of the parabolic mirror and simulations to design the crystals for this energy.

3. Beam expander for interferometric measurements

3.1 Introduction

X-ray optics of high precision require innovative methods for their measurements. At INAF-OAB we have developed an interferometric method that, starting from a collimated beam and employing a train of lenses, in the end will produce a large cylindrical wavefront beam to characterize the shape of Wolter-I optics. Once the errors will be known, it will be possible to correct them for example by means of the Ion Beam Figuring technique, available at INAF-OAB.

The system is composed by:

- 1) A He/Ne interferometer with an exit collimated beam of 100 mm in diameter
- 2) A beam expander composed by three spherical lenses that expand the 100mm beam to a diameter of 300 mm with high accuracy.
- 3) A cylindrical master, composed by three cylindrical lenses having dimensions of 210x60mm, that convert the 300 mm collimated beam to a cylindrical beam having height of 200 mm and with an $F/\text{num}=2.0$

The overall setup of the components is shown in Fig. 17. The 100 mm collimated beam of the interferometer will enter in the Beam Expander tube where the three lenses will expand it to 300 mm. This beam will then illuminate the cylindrical master composed by three cylindrical lenses that will generate a high-quality cylindrical beam with an F/number of 2.0.

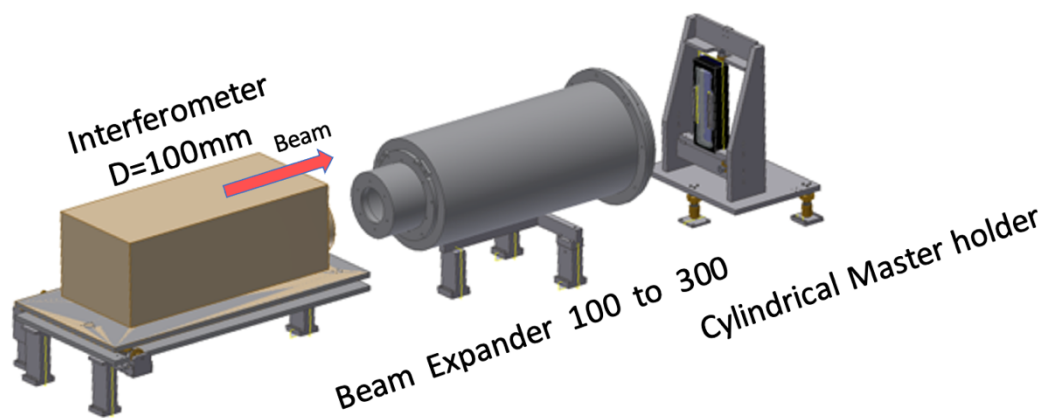


Fig. 17. Setup of the cylindrical measuring system

To measure a Wolter-1 grazing incidence mirror (in pseudo-conical configuration) the cylindrical master lens is tilted with respect to the optical axis so to convert the cylindrical beam into a conical beam that is then sent onto the surface to be measured and reflected back to the interferometer.

The final accuracy of the system will be of the order of 10 nm rms enabling the measurement, correction and production of high-resolution X-ray optics.

In this report we present what has been done and what is planned for the 2022.

3.2 Performed activities

3.2.1. Manufacturing of the Mechanical Components

The system is composed by three mechanical units that consist in:

- The support of the Interferometer that permits its fine alignment with the Beam Expander
- The tube of the Beam Expander that holds the three spherical lenses. The first entrance lens has a diameter of 110 mm, the second inner lens with a diameter of 170 mm and a third last lens with a diameter of 310 mm. From this lens exit the expanded collimated beam with a diameter of 300 mm.
- The holder of the Cylindrical Master that permits its alignment with respect to the collimated beam and generate the cylindrical wavefront.

The next figures present the drawings of these components (Fig. 18) and their physical realization (Fig.19).

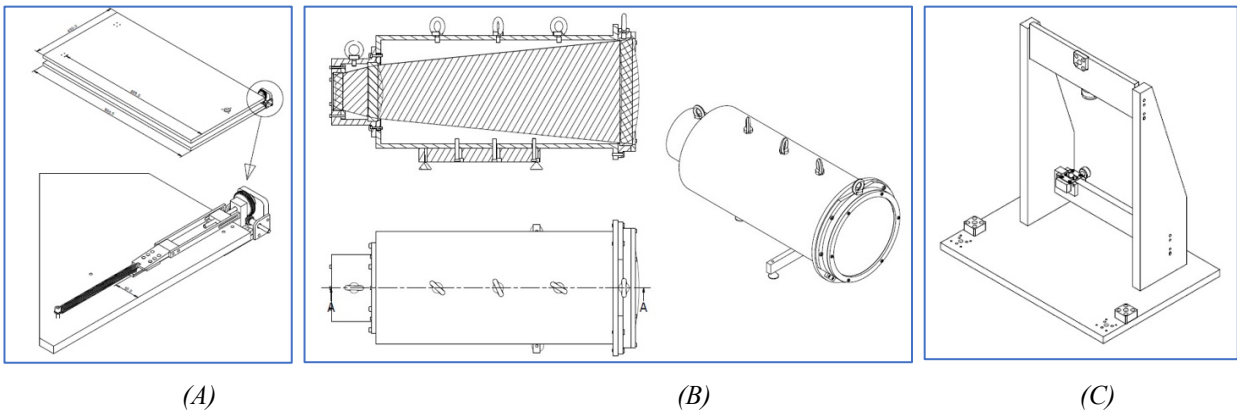


Figure 18: Drawing of the interferometer support (A), the beam expander tube (B) and the holder for the cylindrical master (C)



Figure 19: Realization of the components presented in Fig. 18

A number of other sub-components, like the frame holding the three cylindrical lenses when assembled (Fig. 20) were also manufactured.



Fig. 20. Frame for the Cylindrical Master

A kinematic magnetic holder for a 30 mm mirror has been procured (Fig. 21). This removable component will be installed on the side of the 100 mm entrance of the beam expander tube and will be used as reference for the alignment of the tube with respect to the interferometer beam.



Fig. 21. Kinematic magnetic 30mm mirror holder

We have realized that the support of the Beam Expander tube already fabricated did not include all the necessary degrees of freedom for a quick alignment with the interferometer. Therefore, an upgrade of (Fig. 22) was designed and it is already under realization.

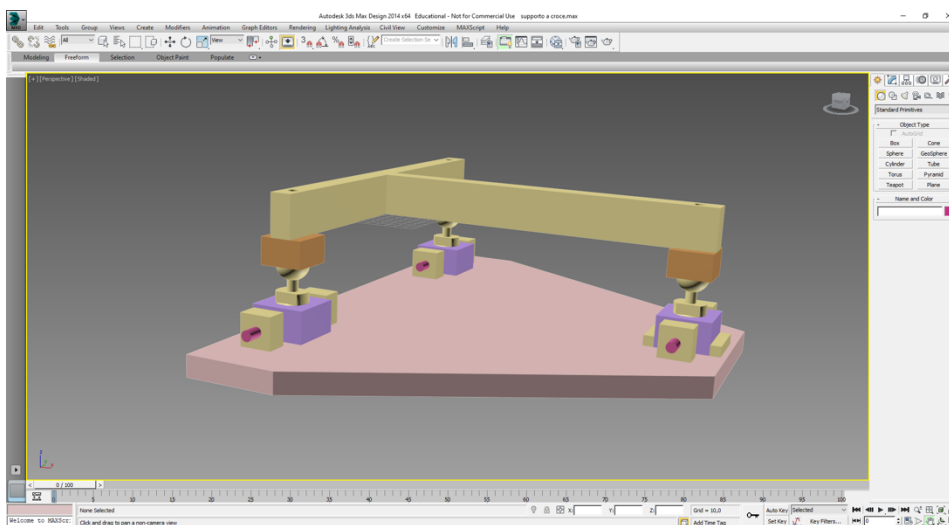


Fig. 22. Improved support of the Beam Expander tube

3.2.2. Measurements of the Beam Expander optical train before IBF

The three spherical lenses composing the beam expander have been integrated in the tube and the resulting wavefront error measured with the interferometer using as reference a 310 mm flat mirror having a very high accuracy of 1/20 lambda PV. Since this mirror is considered “perfect” all the errors that are seen are intrinsic to the lenses of the beam expander. This is the error that needs to be corrected by IBF, correcting adequately only one surface, the outermost one of the 310 mm lens. This surface, contrary to all the others, lack of an antireflection coating to permits its IBF figuring. Since the 310 mm lens need to be disassembled, figured with IBF, reassembled and measured, the repeatability for disassembly/reassembly was measured multiple times: the contribution is estimated to be 20 nm as upper limit, small enough to guarantee the robustness of the process.

To minimize the initial error to be corrected, a set of ring-shaped spacers was built and integrated in the system with the aim to slightly change the separation between the three lenses and reducing the total aberrations. By this approach, the residual error was reduced from 950 to 270 nm rms (Fig. 23B), greatly reducing the IBF figuring time. The IBF figuring of the 310 mm lens surface is one of the activities to be completed.

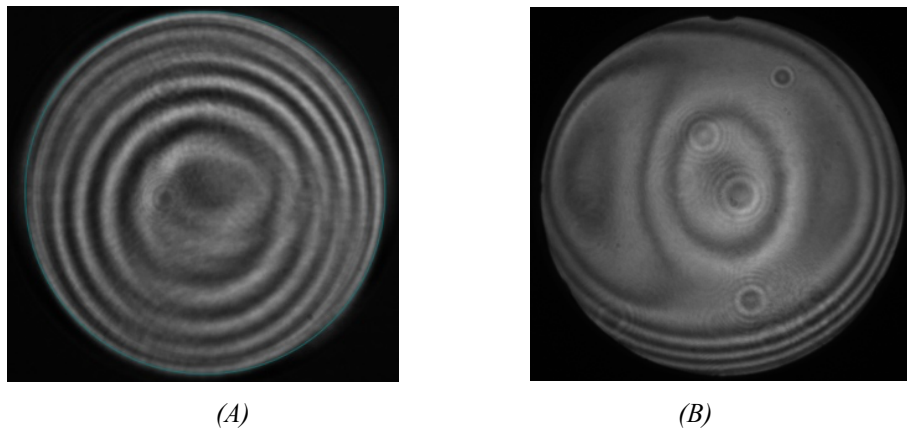


Fig. 23. Comparison of interferograms: A) initial configuration (no spacers), corresponding to 950 nm rms; B) final result, 270 nm rms, which will constitute the starting shape for IBF figure correction

3.2.3. Measurements of the cylindrical lenses with CMC 3D machine

The Master Cylindrical Converter is composed by 3 lenses (Fig. 24,25) and changes the collimated 300 mm beam shape into a cylindrical beam to measure Wolter-1 grazing incidence mirrors. The lenses are made in different materials. Two of the set are done in glass NPH3 (yellow in Fig. 25) and the third (central in Fig. 25) is done in glass TIM28. This combination of materials was chosen to minimize the IBF correction foreseen on one of the surfaces to eliminate the spherical aberration.

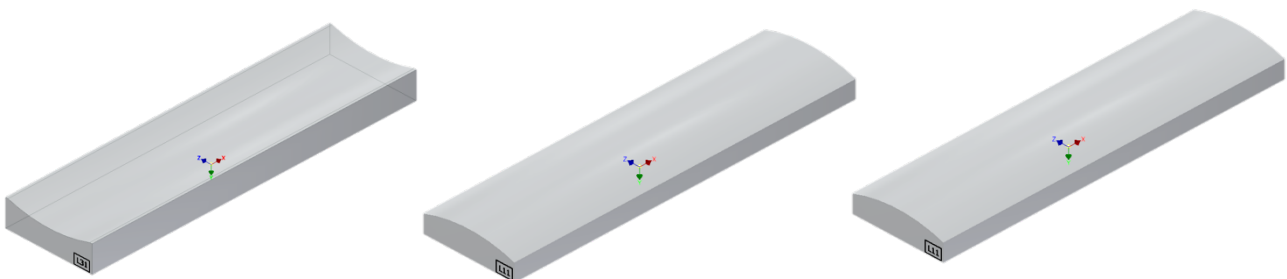


Fig. 24. Drawing of the cylindrical lenses composing the master



Fig. 25. The three lenses composing the cylindrical master

The lenses have been mechanically characterized with the 3D machine operated at OAB, in order to assess their relative mechanical dimensions and their radii of curvature, hence checking the data provided by the vendor. The IBF figuring of these lenses is one of the activities to be completed.

3.2.4. IBF upgrade

Due to the Covid emergency, we had to manage the overlapping of several projects. Some of those required the use of the large IBF head, using a grid set of 50mm or 15 mm; others necessitate the use of a small IBF head, with 30 mm grids and capable to enter in closed, circular mirror shells for their correction. The switching between the two configurations was deemed too much complex to be performed frequently, with the danger of errors in the configurations. In this context, the IBF was upgraded to a system that allows a fast and easy switching of the two heads (Fig. 26), from the electrical and mechanical point of view. Also, the feeding of the Argon gas to the Ion Sources has been split on two lines, managed by means of suitable external valves.

To obtain a stable and performing system in both configurations, the following actions were performed:

- *Completed the electrical separation of the two ion beam heads. This means that the large ion head has now its own neutralizer and the small ion source another one. The latter neutralizer was already available.*
- *The small ion head and its neutralizer are now powered independently from the large one and in particular all the connecting cables has been rebuilt using new single end-to-end cables without connections in between. This has offered the best capability to feed the necessary electrical power using the secondary vacuum feed through that is powering also the neutralizer.*
- *The neutralizer of the small source has been placed closer to the target optical surface, i.e. the walls of the circular shell. This permits to better neutralize the shell wall and avoid the discharge effects observed during the initial tests.*
- *A deep cleaning of all the internal components of the large and small ion heads has been performed to take care of possible contaminating coatings deposited on the ceramic isolators.*

An interesting solution that permits a very fast interchange between the heads has been implemented. Once removing the bridge that hold the small ion head, the latter is hooked up to the internal walls of the vacuum

chamber (Fig. 27) and its internal power cables do not need to be unplugged. During the implementation of the steps described, also the large ion source cables have been renewed changing them with more efficient ones.

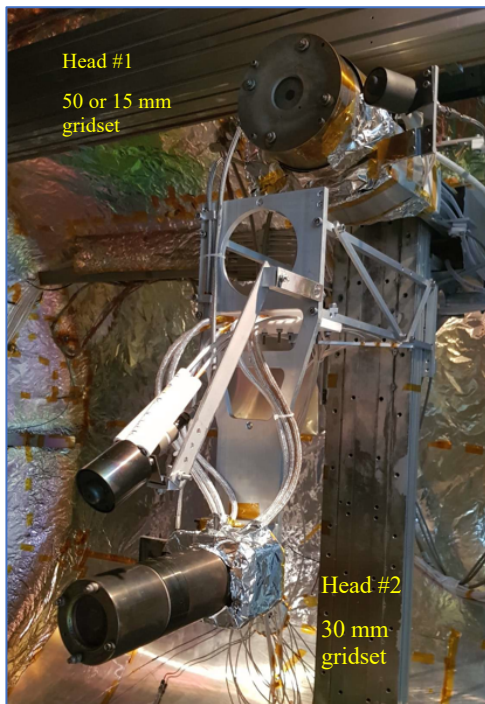


Fig. 26) The IBF after the upgrade

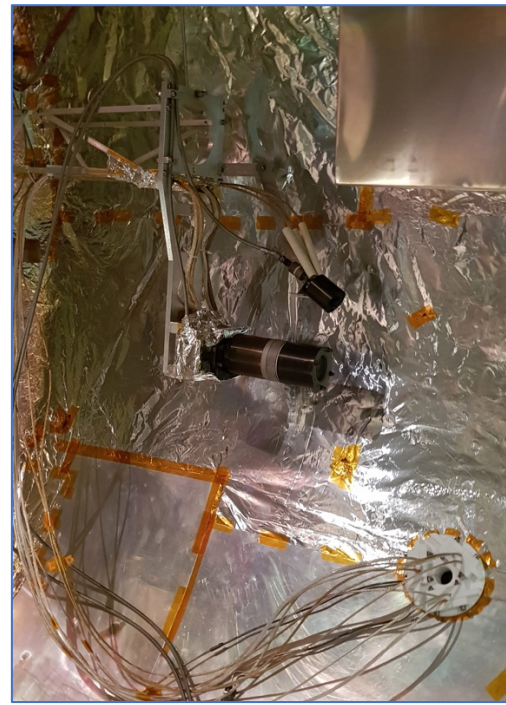


Fig. 27) Small Ion Head hooked up to the inner wall

This system, with two independent ion figuring heads, has been tested successfully. The heads can be switched rapidly, without interfering with each other.

3.3 Programmed activities and schedule

In the next future, the following activities will be performed to complete the metrological system for x-ray optics:

- Complete the system from the mechanical point of view, employing the improved support for the beam expander tube. Another component to be added to the tube is the kinematic magnetic holder for the mirror used for the alignment between the interferometer and the expander itself. The holder for the Cylindrical Master needs to be completed as well.
- Use the Ion Beam Figuring to correct the external surface of the 300 mm lens of the expander in order to obtain a residual error of less of 20 nm rms (a value derived from the repeatability tests done mounting and dismounting the lens, simulating the actions necessary for a number of IBF runs.
- Use the Ion Beam Figuring to correct one of the surfaces of the cylindrical lenses in order to obtain a similar residual error.
- Test of the system and assessment of its performances.

This is expected to be completed by Q4 2022.